Domino Ring Samplers and the new dual readout fiber module

Michele Cascella for the DREAM collaboration

***Abstract*—The dual readout technique consists measuring the electromagnetic fraction of an hadronic shower event by event by comparing the scintillation and Cherenkov light generated in the shower development process.**

Time characteristics of the signals produced by high energy particles in a fiber prototype module are sampled with a commercial VME board based on the Domino Ring Sampler (DRS) chip.

The excellent timing resolution of the DRS-IV based acquisition can be used to recover spatial information on the shower location in a non segmented fiber module. The μs wide buffer opens the possibility of measuring the late neutron component of the hadronic shower.

***Index Terms*—calorimetry, dual readout, DRS, samplers, neutron fraction**

I. Introduction

THE DREAM collaboration has the goal of developing a calorimeter that approaches the theoretical resolution limit in hadronic calorimetry. The dual readout approach consists of measuring event-by-event both the scintillation and Cherenkov light signal and use them to estimate the magnitude of the electromagnetic component of the shower. Dual readout calorimeters can achieve an energy resolution better than $30\%/\sqrt{E(\mathrm{GeV})}$ for hadronic showers.

A. The Dual REAdout Method

Scintillation light (S) is created by any charged particles passing through the sensitive material while Cherenkov light (C) is produced by relativistic particles, i.e. almost exclusively by electrons. The simultaneous measurement of both components can be used to improve hadronic resolution and linearity. The ratio of the two signals can be expressed as a function of f_{em}, the fraction of energy carried by electromagnetic particles in a hadronic shower

$$\frac{C}{S} = \frac{f_{em} + \lambda_C(1 - f_{em})}{f_{em} + \lambda_S(1 - f_{em})} \qquad (1)$$

λ_C and λ_S are the h/e ratios for the material that produces respectively the Cherenkov and the scintillation signal. This equation can be inverted to determine the value of f_{em}.

The dual readout method has first been tested with the DREAM prototype [1], a sampling calorimeter with copper as the absorber medium, and scintillating and clear fibers as the active medium. The Cherenkov light produced in the high density clear fibers is read out separately.

Michele Cascella is with the Department of Physics, INFN and University of Pisa, Italy, e-mail: cascella@pi.infn.it.

The dual readout method has also been tested in high-Z crystals such as PbWO_4 (lead tungstate), BGO (bismuth germanate) and BSO (bismuth silicate). These crystals produce a significant amount of Cerenkov light which can be separated from the scintillation light by exploiting differences in time structure, directionality, spectral properties and polarization.

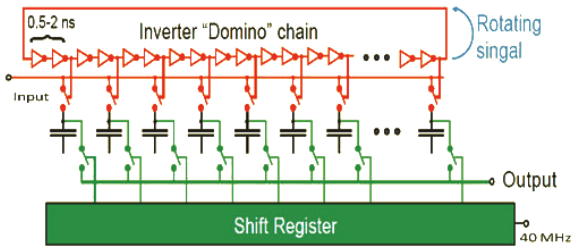

Figure 1. Simplified schematics of the DRS chip.

II. The Domino Ring Sampler chip

The DRS-IV chip [2] is the first multichannel sampler which offers both a very fast sampling and a wide buffer.

The general principles of operations of the DRS-IV chip are the following: a sampling frequency in the GHz range travels in a circular fashion trough a chain of inverters. The analog input signal is stored in an array of 1024 switched capacitor. A trigger signal stops the running "domino wave", freezing the charge in the sampling capacitors. The individual cell contents are then readout by a shift register and digitized outside of the chip. A scheme of the inner workings of the DRS chip is shown in figure 1.

Due to its capability to sample a time profile analysis over relatively large time windows (from 1 μs to 200 ns for sampling frequencies of 1 GSample/s to 5 GSample/s), the DRS chip was first considered in the DREAM project for dual-readout calorimetry to measure the fraction of kinetic energy carried by neutrons produced in hadronic showers.

The first results were obtained with a DRS-II based DAQ system adapted from a trigger board of the MAGIC experiment. These results were cross checked with a Tektronix digital oscilloscope [3], [4], [5].

The most recent version of the DRS chip implements relevant improvements with respect to the previous versions. The intrinsic bandwidth for analog inputs is above 900 MHz, maximum output non-linearity is 0.4 mV for differential analog inputs in the range [-0.5 V, +0.5 V], and thermal drifts of the offset are below 0.1mV/C at room temperature. All these features, and mainly the large bandwidth and the wide

sampling time window, make DRS-IV a device flexible and suitable to process the signals generated by particle showers interacting in dense doped crystals or in fiber calorimeters. Time profile analysis of the readout pulses can be used to

- separate the fast Cherenkov and the slower scintillation components of the light signal produced by particles interacting in dense crystals
- determine the depth at which light is produced in fiber calorimeters
- measure the contribution of neutrons to the hadronic signals from large fiber calorimeters.

The first topic is discussed in detail in this proceedings by [7], [6]. We will present some preliminary results on the two latter topics obtained with a single Pb/fiber prototype module.

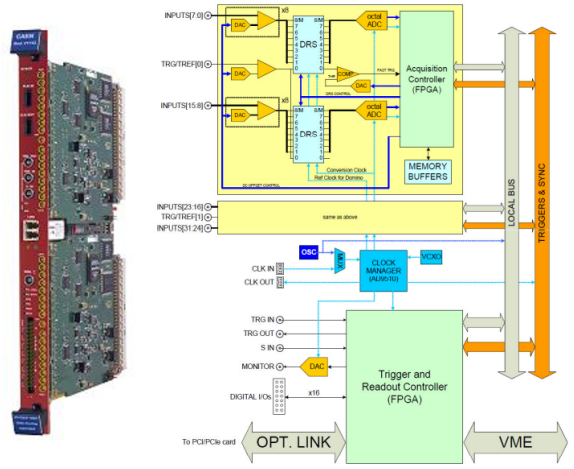

Figure 2. Picture (left) and block schematic (right) of a V1742 digitizer board.

III. The V1742 digitizer board

Since 2010 we have included in our experimental setup a 32 channels CAEN[1] V1742 VME digitizer based on the DRS-IV chip.

The V1742 architecture (shown in figure 2) is similar to that of most CAEN digitizer boards: the motherboard mounts two daughter cards each of them with 16 analog single-ended (50 Ohm) channels connected to two DRS-IV chips and an additional trigger input which is split and fed to the analog trigger input of the two DRS chips.

The daughter boards host a 12-bit flash ADC and a FPGA used to distribute the control signals to the chips, to set the chip input dynamic range via a DAC, to manage the data conversion, and to control the data transfer via an internal bus. External triggers and synchronization signals are passed via internal bus from the motherboard to the daughter boards; The motherboard (which hosts another FPGA) controls the readout transfer via VME bus or optical link. A more complete description of the board can be found on the web [8].

Sampling frequency was set at 5 GS/s, the effective bandwidth of the system is estimated to be larger than 500 MHz, as confirmed by a separate laboratory tests carried out using a waveform generator.

[1]CAEN S.p.A. Viareggio - Italy

IV. The experimental setup

The DREAM collaboration is building a new fiber calorimeter with the aim to improve the performance over the original DREAM detector. This new calorimeter will have a modular design, a sampling fraction of 5% (to be compared to the 2.6% of the DREAM prototype), Cherenkov fibers with larger numerical aperture (resulting in at least a factor 2 improvement in the number of photoelectrons). The assembled newDREAM detector will be larger than the DREAM calorimeter to ensure 99% containment of hadronic showers.

Several design options are under consideration for a number of characteristics: the absorber material (either lead or copper), the structure and construction method of the absorber plates (extrusion, grooving or profiling) and the module size.

Two prototype modules have been assembled so far and their characteristics have been tested at CERN on the H8 test beam line.

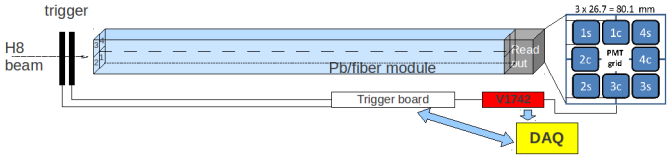

Figure 3. Experimental setup of the fiber detector module at the H8 test beam.

A. The new Pb/fiber prototype module

In the following sections we will present some preliminary results obtained with our second prototype module made of a wafer of $250 \times 89.4 \times 0.1\,\mathrm{cm}^2$ lead plates extruded with grooves designed to house alternate layers of scintillating (Kuraray[2] SCSF-78 with numerical aperture $n = 1.653$) and clear (Mitsubishi[3] Clear SK-40, $n = 1.493$) fibers. At the rear end of the modules Scintillating and clear fibers are bundled separately in groups dividing the module in 4 square towers with a side of 44.7 mm.

The fiber bundles are coupled to the readout PMTs via optical cookies. The four scintillating fiber bundles are readout with standard Hamamatsu[4] R8900 PMTs while clear fiber are readout with R8900-100 PMTs with super bi-alkali photocathodes to enhance quantum efficiency in the UV range. A schematic of the experimental setup is pictured in figure 3.

Our coordinate system has the x axis pointing upward, the y axis parallel to the floor and the z axis along the direction of the beam. The prototype module is mounted on a moving platform (shown in figure 4) that can rotate the module by up to $90°$ with respect to the direction of the beam and position it on the beam transverse plane (the $x-y$ plane) with a precision of 0.5 mm. Most of the measurements were taken with the

[2]Kuraray Co., LTD., Japan
[3]Mitsubishi International Corp., Japan
[4]Hamamatsu Photonics K.K., Japan

beam impinging on the center of the front of the module and with the module placed at a very small angle (1°) with respect to the direction of the beam to avoid the possibility of a particle "channeling" inside one of the fibers. The four calorimetric towers of the module have been equalized and calibrated with an electron beam.

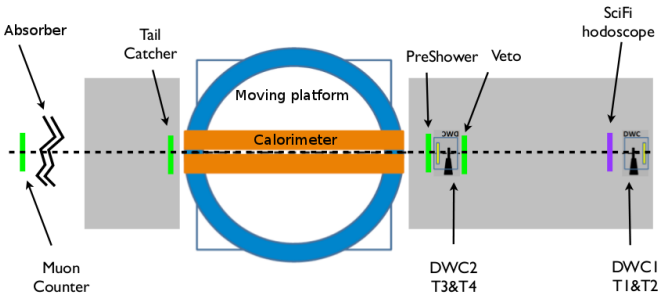

Figure 4. Top view of the placement of the ancillary detectors on the beam line.

B. Ancillary detectors

A number of ancillary detectors are placed on the beam line to provide additional information. The x and y coordinate of the incoming particles are measured using two Delay Wire Chambers (DWC). A preshower detector made of a thin lead plate followed by a scintillator is used to separate electrons from pions. Finally two scintillators are placed in downstream of the calorimeter, a tail catcher is positioned right after the readout system ad is used to tag hadronic showers that are not longitudinally contained in the detector, a second one is placed after a thick block of absorber and is used to identify muons. Figure 4 shows the placement of the different ancillary detectors with respect to the beam line.

In the following analysis the wire chambers have been used to select a small beam spot of $2 \times 2\,\mathrm{cm}^2$, and the other scintillators are used to select a pure sample of the desired particle type.

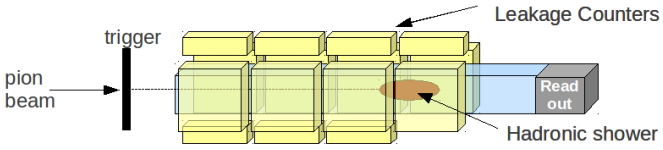

Figure 5. Experimental setup of the prototype module module showing the position of the leakage scintillator blocks.

During most of the data taking the module was surrounded a number of blocks of scintillating material to estimate the amount leakage. The counters are 25 kg, $50 \times 48 \times 10\,\mathrm{cm}^3$ blocks of scintillator recovered form the SHINE experiment arranged in four arrays placed on each side of the module along its length (see figure 5). Each array is made of four counters, with the exception of the bottom array, that only had three counters. The response of each leakage scintillator has been calibrated to the electromagnetic scale with a beam of 180 GeV muons.

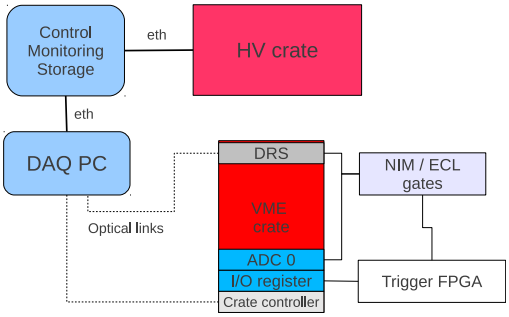

Figure 6. A scheme of the DREAM data acquisition system.

C. The trigger and DAQ system

The trigger is provided by the coincidence of two small scintillators vetoed by third scintillator with a 2 cm diameter hole in the center. The shaped output of the trigger scintillators is fed to an Xilinx[5] Spartan-3AN FPGA Starter Kit that handles the trigger and busy logic and the communication with the DAQ system. The trigger generated by the FPGA logic is sent to several CAEN V792 charge integrating ADC that digitize the output of the ancillary detectors and to the V1742 digitizer that acquires the output of the calorimeter PMTs.

All VME modules are readout via a VME-PCI optical link bridge with the exception of the V1742 is readout through its own dedicated (proprietary) optical link that provides optimal transfer speed. A separate PC is used to start and stop the data acquisition, control the high voltage power supply and for monitoring and storage tasks. A scheme of the DREAM test beam DAQ system can be seen in figure 6.

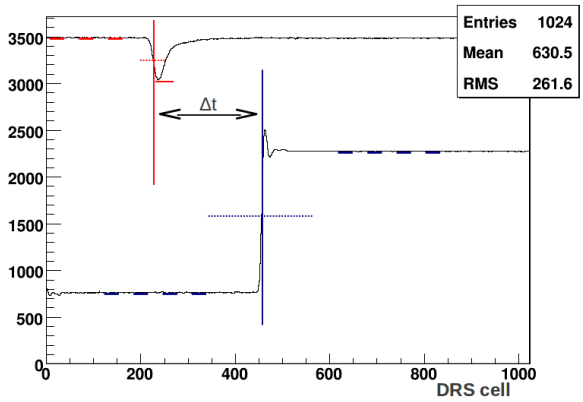

Figure 7. Time profile of a PMT (upper curve) compared to the sampled trigger signal (lower curve).

V. Timing and Longitudinal Positioning Measurements

Figure 7 shows the average time profile of one PMT signal and of the NIM trigger signal sampled by the DRS-IV chip. To correct for the jitter in the sampled signal the timing of the physic signal Δt is defined as the temporal distance between

[5]Xilinx Inc. San Jose, CA, U.S.A.

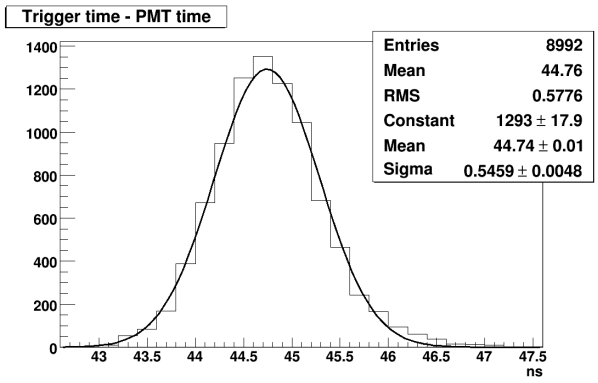

Figure 8. Distribution of Δt for 80 GeV electrons impinging on the front of the module.

the half-height of the trigger signal rising edge and the half-height of the PMT signal.

The distribution of Δt measured with Cherenkov light for electrons impinging on the front of the newDREAM module is shown in figure 8. The measured distribution implies a time resolution of 0.55 ns. Similar results have been obtained in the scintillation channel. A possible contributions to this width is the intrinsic jitter of a trigger obtained with the coincidence of two analog signals of different amplitude.

After placing the module at a an angle of $30°$ with respect to the electron beam the we scanned it with the beam long its z axis at intervals of 10 cm. Comparing the delay at different positions we were able the the speed of light in the fibers.

We obtain a value of $n = 1.63$ for the clear fibers, 8% larger than the nominal value; the discrepancy can be attributed to a small error in the orientation of the $x - y$ moving table with respect to the particle beam.

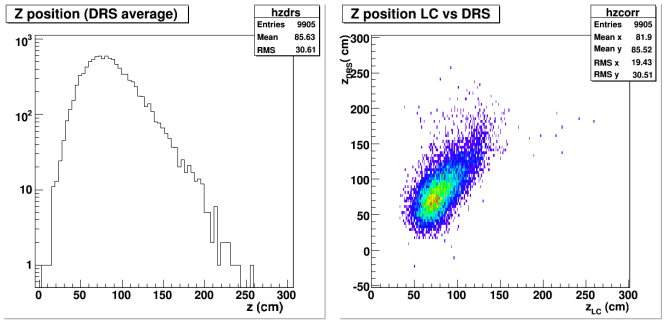

Figure 9. Distribution of z_{DRS} the longitudinal coordinate of the shower maximum determined using delay measurements (left). Scatter plot of of z_{DRS} as a function of z_{LC}, the position determined using the arrays of leakage counters (right).

A. Measurement of the longitudinal position of the shower maximum

A precise determination of the PMT signal delay can be used to measure the longitudinal position of the maximum of an hadronic shower, before the beginning of the shower the particles travel trough the module at the speed of light, much faster than the signal in the fibers. This means that the longer the delay the longer is the length the light has traveled in the fibers and the closer to the module front the particle was when it started showering. The relationship between the measured delay and the position of the shower maximum is the following

$$z_{DRS} = a + b\Delta t \tag{2}$$

where a depends on the geometry and on the signal and trigger cables setup and b is a function of the signal speed in the fibers, both parameters can be determined experimentally.

In our setup we can also estimate the position of the shower maximum by measuring z_{LC}: the barycenter of the signal measured in the leakage counters. The resolution of a single array of four counters is $\Delta z_{LC} = 12$ cm, determined by comparing it with the other arrays. The combined average of all arrays is expected to be better than that.

We have determined the value of a and b by comparing z_{DRS} with z_{LC} in the central region of the arrays ($75 < z_{LC} < 125$) to avoid nonlinearities in the region close to the edge of the arrays. We computed the average value of z_{DRS} in bins of z_{LC} and fitted the result with a straight line to obtain a and b.

Figure 9 shows the distribution of z_{DRS} and the relation between z_{DRS} and z_{LC}. The two methods agree very with each other. The distribution of the difference $z_{DRS} - z_{LC}$ is plotted in figure 10, it has a with of 20 cm pointing to a resolution of the timing method alone between 16 and 18 cm[6], in good agreement with what we expect form a timing resolution of 0.55 ns.

The ability to measure the position of the shower maximum can be used to correct for the effect of light attenuation in the scintillating fibers and thus address an important remaining contributing factor to the measured energy resolution.

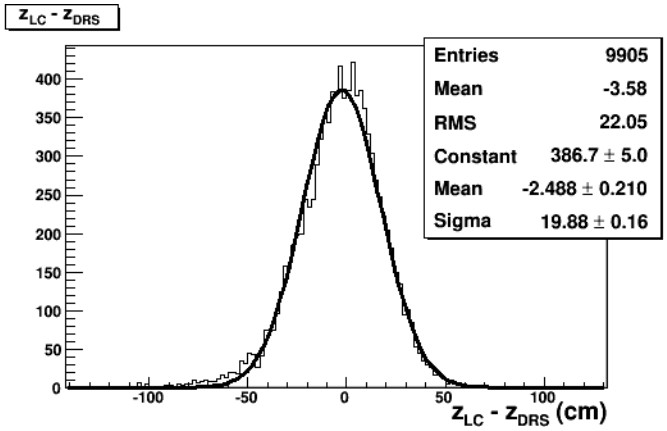

Figure 10. Distribution of the difference $z_{DRS} - z_{LC}$ the width is 20 cm.

VI. Event by event measurement of the neutron fraction

In this section we present some preliminary results on the determination of the slow neutron component in the PMT signal. This technique has already been tested on the DREAM prototype [4], [5] with promising results. Figure 11 shows the

[6]The two estimates results from assuming a resolution on z_{LC} of respectively 12 and 8 cm.

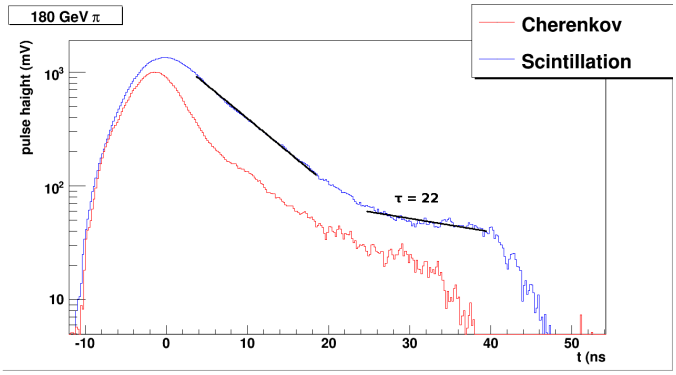

Figure 11. Pulse shape for a single event of a 180 GeV pion hitting the center of the tower for the scintillating fibers (top curve) and the Cherenkov fibers (bottom curve). The scintillation signal is fitted with an exponential distribution in two different regions.

PMT pulse shape for the scintillating and clear (Cherenkov) fibers of the same tower of the prototype module hit by a 180 GeV pion.

While the main component is clearly visible in both channels a second slow component with a characteristic time of $\tau \sim 22$ ns is clearly visible in the hydrogen rich scintillating fibers while it is absent in the Cherenkov fibers.

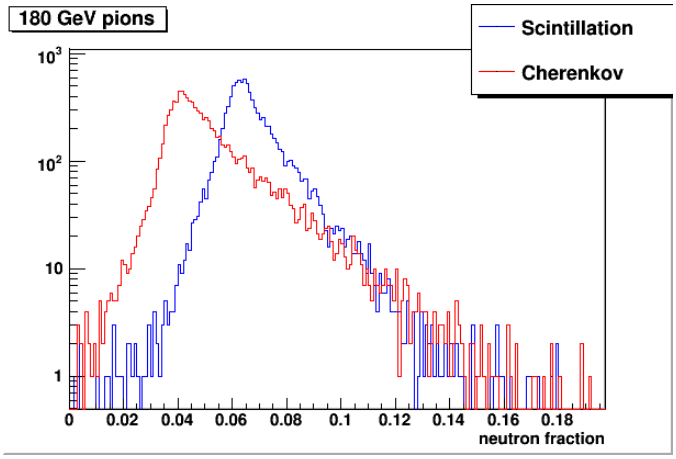

Figure 12. Distribution of f_n measured in the scintillating (blue) and Cherenkov (red) fibers with a beam of 180 GeV pions hitting the center of the tower.

To estimate the fraction of the shower energy carried by neutrons we have decided to look at the integral of the scintillation signal between 20 and 40 ns after the signal peak. The neutron fraction is defined as follows:

$$f_n = \frac{\int_{t=20\text{ns}}^{t=40\text{ns}} S\,dt}{\int S\,dt} \qquad (3)$$

where S is the signal in the Scintillating fibers, this definition is analogous to that of [5]. Figure 12 shows the distribution of f_n in scintillating and Cherenkov fibers measured for a beam of 180 GeV pions hitting the center of the tower. Our variable f_n is markedly larger in scintillating fibers that capture a larger fractions of neutrons. The difference between the two channels can be used to estimate the fraction of shower energy energy carried by neutrons.

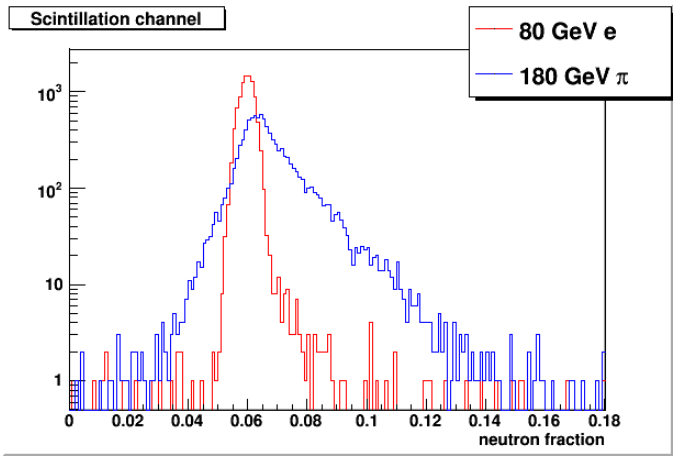

Figure 13. Distribution of f_n measured in the scintillating fibers with a beam of 80 GeV electrons (red) and 180 GeV pions (blue) hitting the center of the tower.

The distribution of f_n measured in scintillating fibers with 180 GeV pions is compared with the distribution of the same variable measured with a beam of 80 GeV electrons in figure 13. As expected the average value is much larger for pions than for electrons, with the pion distribution being much broader and with a larger tail at high f_n.

VII. Conclusions

In this paper we have presented several preliminary results obtained with a commercial VME board equipped based on the DRS-IV chip. We have given a short description of the prototype Pb/fiber module, of the experimental setup and of the DAQ system.

The ability to measure the timing of a particle induced shower with a resolution of 0.55 ns translates into the possibility of determining the position of the shower maximum in a non segmented hadronic calorimeter with a precision of 16 to 18 cm.

We are also exploring the possibility to measure event by event the fraction of energy carried by neutrons in an hadronic shower. Our preliminary results show that we can indeed separate and measure the signal associated with the slow neutron component in an hadronic shower and we plan to test this technique with our final calorimeter setup to further reduce the hadronic resolution of the detector.

References

[1] N. Akchurin, et al., Nucl. Instr. and Meth. A 533 (2004) 305; N. Akchurin, et al., Nucl. Instr. and Meth. A 536 (2005) 29; N. Akchurin, et al., Nucl. Instr. and Meth. A 537 (2005) 537; N. Akchurin, et al., Nucl. Instr. and Meth. A 548 (2005) 336; N. Akchurin, et al., Nucl. Instr. and Meth. A 550 (2005) 185.
[2] S. Ritt, et al., Nucl. Instr. and Meth. A 623 (2010) 486.
[3] R.Wigmans, Nucl. Instrum. Meth. A 572 (2007) 215. N. Akchurin et al., Nucl. Instrum. Meth., A 584 (2008) 273-284.
[4] J. Hauptman, Estimate of neutrons event by event in DREAM, Proceedings of CALOR08 conference, (2008)
[5] M. Incagli, DREAM Collaboration, Nuclear Science Symposium Conference Record, 2008. NSS '08. IEEE, 19-25 Oct. 2008, pages 1673 - 1677.
[6] S. Franchino, Dual-Readout Calorimetry with a Mo-Doped $PbWO_4$ Electromagnetic Section, this volume.

[7] D. Pinci, BGO-Based Electromagnetic Section for a Dual Readout Calorimeter, this volume.
[8] http://www.caen.it/csite/CaenProd.jsp?idmod=661&parent=11

Michele Cascella Is a post doctoral fellow at University of Pisa.